

# Non-Isothermal Kinetics of Water Adsorption in Compact Adsorbent Layers on a Metal Support

G. Földner<sup>\*1</sup>, L. Schnabel<sup>1</sup>

<sup>1</sup>Fraunhofer Institute Solar Energy Systems, Freiburg

<sup>\*</sup>Corresponding author: Heidenhofstr.2, 79110 Freiburg, gerrit.fueldner@ise.fraunhofer.de

**Abstract:** Water adsorption in highly porous materials can be used in heat transformation processes for the efficient use of energy in heat and cold production [8]. To optimize the power density of compact thin layer adsorbent beds, a one-dimensional model of the coupled heat and mass transfer limiting the adsorption kinetics has been set up in COMSOL Multiphysics. Results which are presented in this paper have been validated and calibrated with measurements.

**Keywords:** water adsorption kinetics, heat transfer, Knudsen diffusion

## 1 Introduction

Thermally driven chillers and heat pumps use heat from a high temperature heat source (solar or waste heat, gas burner) to efficiently supply heat at a medium temperature level (heat pump) or cold at a low temperature level (chiller). One technology for such a thermal heat transformation is the use of water adsorption in highly porous adsorbents like zeolite [8]. Adsorbents used in such a machine are made up of a heat exchanger fluid loop in contact with an adsorbent bed. The volume specific power density [ $\text{W}/L_{\text{machine-volume}}$ ] of such machines is limited -besides the maximum water uptake of the used adsorbent- by the coupled mass transfer (water vapour) into the adsorbent and heat transfer (heat of adsorption) to the fluid loop, see Figure 1 for a schematic drawing. To compare different new adsorber concepts, small samples ( $50 \times 50 \text{ mm}^2$ , see Figure 2) representing a part of such an adsorber are characterized experimentally at Fraunhofer ISE. Measurements are performed in a constant volume set-up, where the decrease in system pressure can be directly converted into water uptake of the adsorbent material. The exper-

imental setup is explained in more detail in section 2.

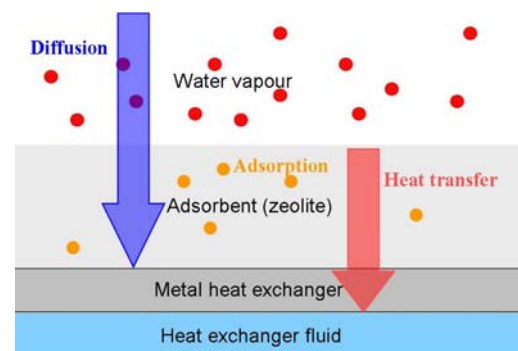


Figure 1: Coupled heat and mass transfer in a compact adsorber heat exchanger

A one dimensional model of the coupled mass and heat transfer has been set up within COMSOL Multiphysics and has been validated with experimental data in order to identify the limiting factors for the adsorption kinetics and to optimize such samples with respect to layer thickness, coupling to heat exchanger or other parameters.

## 2 Experimental setup

The sample characterised experimentally consists of a more or less homogenous layer of zeolite (UOP DDZ 70) with a thickness of 0.72 mm which is glued onto an aluminum support with a thickness of 3 mm. Between this sample and a coldplate kept at constant temperature by a thermostat, a Captec heat flux sensor is attached with heat conducting paste. The experimental setup is shown in Figure 2.

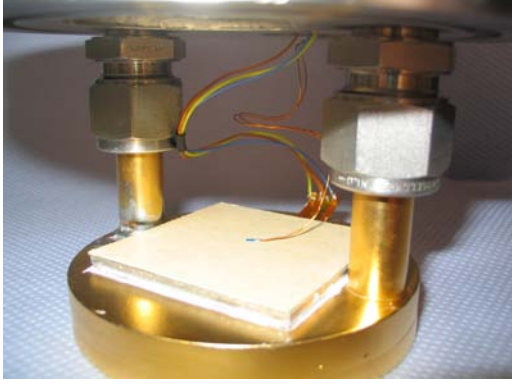


Figure 2: Sample (50x50 mm<sup>2</sup>) with aluminum carrier on coldplate with temperature and heat flux sensor.

The sample is desorbed at 95 °C against vacuum pump pressure (1 Pa). After cooling down the sample to 40 °C, a valve is opened between a big dosing chamber containing water steam at 40 °C at a pressure of about 1700 Pa and the sample chamber; the sample starts to adsorb, releasing the heat of adsorption, until adsorption equilibrium is reached.

### 3 Model description and implementation

Due to symmetry reasons the mathematical model is one-dimensional. It includes diffusion of water vapour into the adsorbent layer, the adsorption process and heat transfer by conduction within the adsorbent and metal layer. Additionally, the following assumptions are made:

- Adsorption equilibrium is reached at each place and time instantaneously, depending on local pressure and temperature.
- Water vapour is described as an ideal gas (see Eq. (9)).
- Heat transfer by convection inside the open pore volume is ignored.
- The fluid loop is included only by a constant temperature boundary.

To comply with the measuring procedure, the time-dependent form of the PDE's is used since the process is not stationary.

A comprehensive overview on adsorption technology and the mathematical description of adsorption kinetics can be found in

[7]. A detailed model description of the model used in this work is given in [11]. Other related material used in the derivation of this model are the publications [1],[2], [3], [5] and [9].

#### 3.1 Mass balance

The equation governing the mass transfer of water vapour inside the adsorbent layer can be derived from a simple mass balance and reads

$$\frac{\partial c_{Ad}}{\partial t} = \frac{\partial}{\partial z} D \frac{\partial c_{Ad}}{\partial z} - \frac{1}{M} \frac{\rho_{Ad}^{dry}}{\psi} \frac{dX}{dt} \quad (1)$$

It includes the process of adsorption as a sink term.  $c_{Ad}$  is the water vapour concentration in [mol/m<sup>3</sup>],  $D$  is the diffusion coefficient [m<sup>2</sup>/s],  $\rho_{Ad}^{dry}$  the density of the dry adsorbent in [kg<sub>Ad</sub>/m<sup>3</sup>] corresponding to the layer volume,  $M$  the molar mass of water in [kg/mol],  $\psi$  the adsorbent porosity and  $X$  the water loading in [kg<sub>H2O</sub>/kg<sub>Ad</sub>].

The equation in the pure vapour area is a standard Fickian diffusion equation with a diffusion coefficient  $D_v$  which is about two orders of magnitude higher than the diffusion coefficient  $D$  within the adsorbent. For comparison the boundary and initial conditions are set equal to those given by the experimental set-up:

- At  $t = 0$ , the adsorbent is at a very low pressure (vacuum pump ending pressure 1 Pa); a given amount of water vapour is then dosed into the vapour chamber (initial pressure at boundary 4, see Figure 3), leading to a jump in pressure there. To avoid numerical problems caused by too steep gradients in pressure and temperature, a smoothed Heaviside function is used as initial condition as well as for the diffusion coefficient to model the concentration front reaching the adsorbent surface.
- The boundary condition at boundary 3 (see Figure 3) is given by "concentration", the concentrations  $c_{Ad}$  and  $c_v$  being equal at each timestep. On boundary 4, the boundary condition is given by a normal flux which is proportional to the change in concentration on the vapour side.

The exact boundary conditions are given in Table 2.

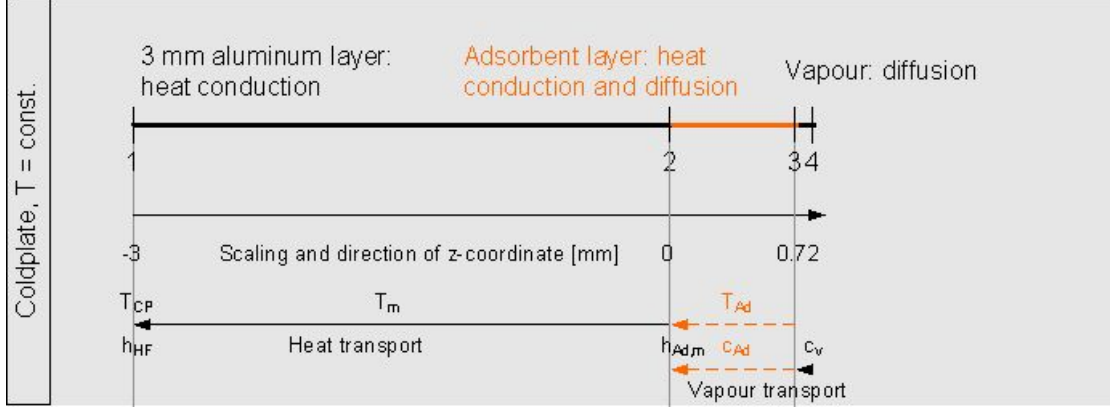


Figure 3: Geometry and boundaries in COMSOL

### 3.2 Energy balance

The energy balance within the adsorbent includes the heat of adsorption released in the adsorption process as a heat source,

$$\rho_{Ad}^{dry} c_{p,Ad} \frac{\partial T_{Ad}}{\partial t} = \bar{\lambda}_{Ad} \frac{\partial^2 T_{Ad}}{\partial z^2} + \rho_{Ad}^{dry} h_{ad} \frac{dX}{dt} \quad (2)$$

where  $c_{p,Ad}$  is the specific, loading dependent adsorbent heat capacity [J/(kg K)],  $\bar{\lambda}_{Ad}$  the loading dependent heat conductivity of the adsorbent [W/(m K)] and  $h_{ad}$  the specific enthalpy of adsorption [J/kg<sub>H2O</sub>] which is calculated according to Eq.7. Within the metal layer, heat transfer takes place by conduction with the library values for standard aluminum. To avoid numerical problems because of steep temperature gradients in the beginning, the variable transformation

$$T_{Ad,log} = \ln T_{Ad} \quad (3)$$

is used and the differential equation is solved for  $T_{Ad,log}$ . The initial and boundary conditions are given by the experimental set-up:

- The initial temperature is for all regions the same and corresponds to the coldplate temperature.
- At boundary 3 "thermal insulation" is defined; heat losses by radiation and convection are ignored.
- At boundary 2, the boundary condition is "heat flux" with a heat transfer coefficient  $h_{Ad,m}$  and the two temperatures  $T_{Ad}$  and  $T_m$ .
- At boundary 1 - due to heat flux measurements - a second heat transfer resistance exists, therefore "heat flux"

is defined by the heat transfer coefficient  $h_{HF}$  and the temperatures  $T_m$  and  $T_{CP}$ , which is the constant temperature of the cooling fluid loop.

The variable transformation also has to be carried out for the boundary and initial condition, so e.g. the thermal conductivity gets an extra factor of  $\exp(T_{Ad,log})$ , with the time scaling coefficient  $\delta_{ts} = \exp(T_{Ad,log}) = T_{Ad}$ . The exact formulations are given in Table 2.

### 3.3 Adsorption equilibrium

Loading equilibrium has been measured for the modeled material (UOP DDZ 70) in a thermogravimetric balance. From this data, a characteristic curve

$$W(A) = \frac{a_1 + a_2 A + a_3 A^2 + a_4 A^3}{1 + a_5 A + a_6 A^2 + a_7 A^3} \quad (4)$$

has been fitted using a generalized form of Dubinin's theory of volume filling [4, 10], where  $W = X/\rho_{H2O}$  [cm<sup>3</sup>/kg<sub>Ad</sub>] is the filled volume per adsorbent mass (the adsorbate density is taken equal to the density of liquid water) and

$$A = \frac{RT_{Ad}}{M} \ln \left( \frac{p_{sat}}{p} \right) \quad (5)$$

$$= \frac{RT_{Ad}}{M} \left( \ln \left( \frac{p_{sat}}{c_{Ad} R} \right) - T_{Ad,log} \right) \quad (6)$$

is called the adsorption potential [J/g<sub>H2O</sub>],  $p_{sat}$  being the saturation pressure of water at temperature  $T_{Ad}$ . The coefficients  $a_i$  are given in Table 1.

$a_1$	221.16073	$a_5$	-0.002006
$a_2$	-0.790530	$a_6$	-2.224e-6
$a_3$	0.0014848	$a_7$	1.6494e-8
$a_4$	-5.129e-7		

Table 1: Coefficients of characteristic curve  $W(A)$

The enthalpy of adsorption can be calculated using the adsorption potential:

$$h_{ad} = h_{ev} + A \quad (7)$$

where  $h_{ev}$  is the evaporation enthalpy of water at temperature  $T_{Ad}$ . The loading change with time is given by the total differential

$$\frac{dX}{dt} = \left( \frac{\partial X}{\partial p} \right)_T \frac{\partial p}{\partial t} + \left( \frac{\partial X}{\partial T} \right)_p \frac{\partial T}{\partial t} \quad (8)$$

Since the characteristic curve serves as a parameterization of the equilibrium data, the partial derivations of  $X$  in the expression above can be calculated from it. The relationship between  $p$  and  $c_{Ad}$  comes from the

ideal gas law,

$$p = c_{Ad}RT \quad (9)$$

with  $R$  [J/(mol K)] the general gas constant. The properties of water ( $\rho_{H_2O}, p_{sat}, h_{ev}$ ) correspond to the standard data IAPWS-IF97 [6].

### 3.4 Meshing and solver settings

The model has been solved in transient mode for 1200 s with timesteps stored every 0.2 s, so adsorption equilibrium could be reached even in the slowest case. The relative tolerance has been set to  $1e-4$ . A customized mesh has been created, being denser in subdomains 2 and 3 (adsorbent and vapour layer) and coarser in subdomain 1. With a number of 352 elements (1118 degrees of freedom), independency of the solution from the mesh was sufficient to be far below the error bar of the measurement.

	Mass balance	Energy balance
<b>Vapour</b>	$\frac{\partial c_v}{\partial t} = \frac{\partial}{\partial z} D_v \frac{\partial c_v}{\partial z}$	–
Initial	$c(0) = c_0 - (c_0 - c_{Ad0}) * HS$ with $HS = \text{flc2hs}(7.5e-4 - x, 1e-5)$ and $D_v = 0.01 - (0.01 * \text{flc2hs}(3 - t, 3))$	$T(t=0) = T_{CP} = const.$
Boundary	4 : $\mathbf{n}(D_v \nabla c_v) = -\frac{V_{tot}}{\psi_{Ar}} \frac{\partial c_v}{\partial t}$ and 3 : $c_v = c_{Ad}$	
<b>Adsorbent</b>	$\frac{\partial c_{Ad}}{\partial t} = \frac{\partial}{\partial z} D \frac{\partial c_{Ad}}{\partial z} - \frac{1}{M} \frac{\rho_{Ad}^{dry}}{\psi} \frac{dX}{dt}$	$\delta_{ts} \rho_{Ad}^{dry} c_{p,Ad} \frac{\partial T_{Ad,log}}{\partial t} =$ $\bar{\lambda}_{Ad} T_{Ad} \frac{\partial^2 T_{Ad,log}}{\partial z^2} + \rho_{Ad}^{dry} h_{ad} \frac{dX}{dt}$
Initial	$c_{Ad}(t=0) = c_{Ad0} = 1 Pa$	$T_{Ad,log}(t=0) = \ln T_{CP}$
Boundary	3 : $c_{Ad} = c_v$	2 : $\mathbf{n}(\bar{\lambda}_{Ad} T_{Ad} \nabla T_{Ad,log}) =$ $\frac{h_{Ad,m}}{T_{Ad,log}} T_{Ad}$
<b>Metal</b>	–	$\rho_m c_{p,m} \frac{\partial T_m}{\partial t} = \lambda_m \frac{\partial^2 T_m}{\partial z^2}$
Initial	–	$T_m(t=0) = T_{CP}$
Boundary	–	2 : $\mathbf{n}(\lambda_m \nabla T_m) = h_{Ad,m}(T_{Ad} - T_m)$ 1 : $\mathbf{n}(\lambda_m \nabla T_m) = h_{HF}(T_{CP} - T_m)$

Table 2: Governing equations, initial and boundary conditions;  $\mathbf{n}$  is the boundary normal pointing out of the domain

## 4 Results

Figure 4 shows simulated and experimental pressure within the vapour room. As described in section 2, the loading  $X$  can be calculated from this pressure drop when the volume and the dry adsorbent mass are known exactly.

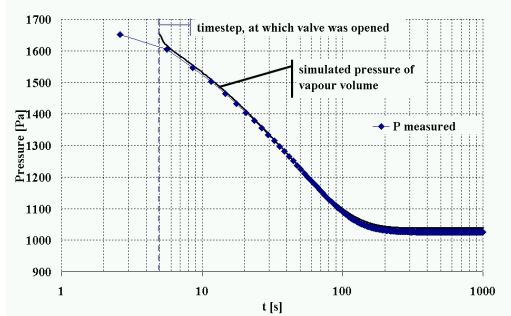


Figure 4: Simulated and experimental water vapour pressure in vapour room

At the same time, when adsorption takes place, the temperature  $T_{Ad}$  within the adsorbent will rise due to the release of adsorption enthalpy  $h_{Ad}$ . Only when the initial temperature is reached again, thermodynamic equilibrium is reached. Figure 5 shows the simulated adsorbent layer surface temperature in comparison to measured results (blue dots).

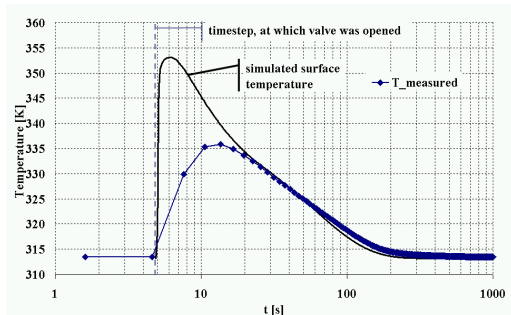


Figure 5: Adsorbent surface temperature

The simulated surface temperature reaches a much higher maximum, and also at an earlier point in time (Figure 6, grey line) than the measured temperature. This is due to a heat flux resistance between the surface and the temperature sensor. Modeling this resistance leads to much better agreement between measurement results and simulation (Figure 6, black lines).

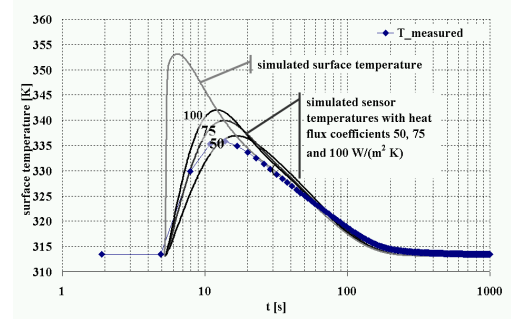


Figure 6: Influence of heat flux resistance of temperature sensor

With the same parameters, also the comparison of simulation results with the heat flux measurement (blue dots) between the metal support and the coldplate shows good agreement (Figure 7).

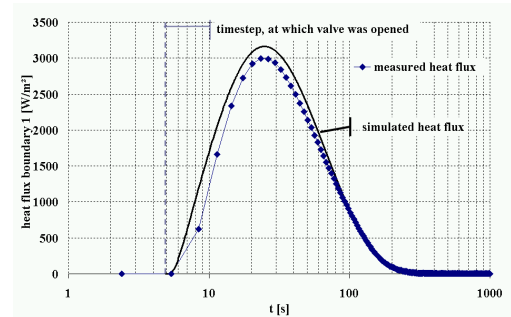


Figure 7: Simulated and experimental heat flux through boundary 1.

The simulated heat flux is slightly higher, since no losses (e.g. by radiation and convection) have been taken into account.

## 5 Conclusion

A 1-d model of water adsorption kinetics in a compact layer of porous zeolite on a metal carrier has been implemented in COMSOL Multiphysics and validated by measurement results. The initial conditions and geometry have been adjusted to real experimental conditions, thus avoiding unphysically steep gradients in vapour concentration and adsorbent temperature and providing for better numerical stability. A transformation to the logarithm of the adsorbent layer temperature is used to minimize numerical errors which turn up using the non-logarithmic form. Simulation results show that the adsorbent surface temperature reached during the adsorption process is actually higher

than the measured temperature due to the dynamic behaviour of the sensor. Therefore, a different way of measuring the surface temperature is proposed (e.g. infrared sensor) to check the simulation results.

The model can now be used for parameter variations to find out possible mass or heat transfer limitations and allowing for optimization of layer thickness or other parameters to obtain higher power densities of adsorbers in heat transformation applications. Results of this optimization process will be presented in future publications.

## References

- [1] D. Bathen and M. Breitenbach, *Adsorptionstechnik*, Springer, Berlin Heidelberg New York, 2001.
- [2] U. Busweiler and W. Kast, *Nichtisotherme Ad- und Desorptionskinetik am Beispiel der Wasserdampfsorption an Einzelkörnern technischer Adsorbentien*, Chem.-Ing.-Tech. **56** (1984), no. 11, 860–861.
- [3] M. Sc. Eng. Belal Dawoud, *Thermische und kalorische Stoffdaten des Stoffsystems Zeolith MgNaA-Wasser*, Ph.D. thesis, Fakultät für Maschinenwesen der RWTH Aachen, 1999.
- [4] M. M. Dubinin, *Adsorption in micropores*, Jour. of Colloid and Interface Science (1967).
- [5] S. Eichengrün, *Theoretische und experimentelle Untersuchung des dynamischen Verhaltens von periodisch arbeitenden Sorptionskälteaggregaten*, Ph.D. thesis, TU München, 1994.
- [6] IAPWS-IF97, *IAPWS Industrial Formulation 1997 for the Thermodynamic Properties of Water and Steam*, 1997.
- [7] W. Kast, *Adsorption aus der Gasphase*, Ingenieurwissenschaftliche Grundlagen und technische Verfahren, VCH-Verlag, 1988.
- [8] F. Meunier, *Solid sorption heat powered cycles for cooling and heat pumping applications*, Applied Thermal Engineering **18** (1998), no. 9-10, 715–729.
- [9] T. Miltkau and B. Dawoud, *Dynamic modeling of combined heat and mass transfer during the adsorption of water vapor into a zeolite layer of an adsorption heat pump*, International Journal of Thermal Sciences **41** (2002), 753–62.
- [10] T. Núñez, H.-M. Henning, and W. Mittelbach, *Adsorption cycle modeling: Characterization and comparison of materials*, ISHPC '99, Proc. of the Int. Sorption Heat Pump Conf., 1999.
- [11] L. Schnabel, *Experimentelle und numerische Untersuchung der Adsorptionskinetik an Adsorbens-Metalverbundstrukturen*, Ph.D. thesis, TU Berlin, 2008 (not yet published).

## Nomenclature

$A$	adsorption potential	[J/g <sub>H2O</sub> ]
$A_r$	sample surface area	[m <sup>2</sup> ]
$D$	pore diff. coeff.	[m <sup>2</sup> /s]
$D_v$	self-diff. coeff.	[m <sup>2</sup> /s]
$M$	molar mass	[kg/mol]
$R$	general gas constant	[J/(mol K)]
$T_{Ad}$	adsorbent temperature	[K]
$T_{Ad,log}$	logarithmic temperature	
$T_{CP}$	coldplate temperature	313.15 K
$T_m$	metal temperature	[K]
$V_{tot}$	vapour chamber volume	[m <sup>3</sup> ]
$W$	filled pore volume	[cm <sup>3</sup> /kg <sub>Ad</sub> ]
$X$	water loading	[kg <sub>H2O</sub> /kg <sub>Ad</sub> ]
$a_i$	coeff. char. curve	
$c_{Ad}$	vapour conc. Ad	[kg/mol]
$c_v$	vapour conc.	[kg/mol]
$c_{p,Ad}$	ads. spec. heat capacity	[J/(kg K)]
$h_{ad}$	spec. ads. enthalpy	[J/kg]
$h_{ev}$	spec. evap. enthalpy	[J/kg]
$h_{Ad,m}$	heat transf. coeff. Ad/m	[W/(m <sup>2</sup> K)]
$h_{HF}$	heat transf. coeff. m/CP	[W/(m <sup>2</sup> K)]
$p$	pressure	[Pa]
$p_{sat}$	water saturation pressure	[Pa]
$\delta_{ts}$	time scaling coefficient	[-]
$\bar{\lambda}_{Ad}$	ads. heat conductance	[W/(m K)]
$\rho_{Ad}^{dry}$	dens. of dry adsorbent	[kg/m <sup>3</sup> ]
$\rho_{H2O}$	dens. of water	[kg <sub>H2O</sub> /cm <sup>3</sup> ]
$\psi$	porosity of adsorbent	[-]

## Acknowledgements

Funding by PhD scholarship of DBU (Deutsche Bundesstiftung Umwelt) to both authors is gratefully acknowledged.